Energy Equip. Sys./ Vol. 5/No . 3/September 2017/ 265-273

ENERGY EQUIPSYS

Energy Equipment and Systems

http://energyequipsys.ut.ac.ir
www.energyequipsys.com

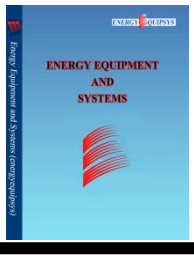

Performance evaluation of trapezoidal teeth labyrinth seal

Authors

Razie Abdous [a]
Saadat Zirak [b*]

[a] Aerospace Department, Semnan University, Semnan, Iran

[b] Mechanical Engineering Department, Semnan University, Semnan, Iran

Article history:

Received : 6 March 2017
Accepted : 24 June 2017

ABSTRACT

The present paper investigates the effects of the trapezoidal teeth labyrinth seal on the leakage amount in gas turbines. The influences of increasing the number of teeth from 1 to 6 with step 1 and the tip clearance s=0.5 to 7.5 mm on the leakage flow at different pressure ratios of PR=1.5, 2 and 2.5 are examined, comprehensively. The analysis is performed numerically using a Finite-Volume software with the k-ε turbulent model. The obtained results show a good agreement in comparison with the other research results. The results show that an increase in the number of teeth causes a decrease in the leakage flow. An increase in the tip clearance (s) from 0.5 mm to around 7.5 mm leads to a decrease in the leakage flow, like the step labyrinth behavior, while an increase beyond 7.5 mm results into a leakage increase, the behavior of the straight labyrinth.

Keywords: Labyrinth, Seal, Trapezoidal, Number of Teeth, Tip Clearance, Leakage Flow, CFD.

1. Introduction

The Labyrinth seals and their sealing rules are in wide use in a variety of configurations in turbomachinery. The straight, interlocking, slanted, stepped and their combinations are the most common of them. By nature, the labyrinth seals are widely mounted in gas and steam turbines [1], particularly in the compressor and the turbine blade tip areas and the secondary air system. Recent designs of gas and steam turbines required accurate knowledge of the flow through the seals.

Stoff [2] numerically examined the incompressible flow in a labyrinth seal using the k-ε turbulence model with a pressure-velocity computer code in order to explain the leakage behavior against the mean pressure gradient. The numerical results were compared with the measurements obtained by a back-scattering laser-Doppler anemometer at a cavity Reynolds number of 3×10^4 and a Taylor number of 1.2×10^4. Rhoded et al. [3], with the implementation of the QUICK differencing scheme into a TEACH-type computer code to calculate the pressure drop for a specified incompressible flow leakage rate in a labyrinth seal. By using the single volume model, Malvano et al. [4] could establish the rotordynamic coefficients of the straight-through labyrinth gas seals. An improved understanding of a new category of the stepped labyrinth seals was presented in the published literature by Rhode et al. [5]. They presented the degree of through flow path penetration into the annular groove, which gives the largest and the smallest leakage resistance improvement over that of the corresponding conventional stepped seal. Vakili et al. [6] investigated in detail the leakage flow in a constant rotor diameter stepped labyrinth seal using the pressure and velocity field measurements and the

*Corresponding author: Saadat Zirak
Address: Mechanical Engineering Department, Semnan University, Semnan, Iran
E-mail address: s_zirak@profs.semnan.ac.ir

numerical simulation of 2-D and axisymmetric models. Kim and Cha [7] numerically investigated the influence of the configuration and clearance on the leakage behavior of the straight and stepped labyrinth seals. They validated their results with analytical and experimental data. The analytic method anticipates higher values of leakage than others. The clearance size showed a considerable effect of the leakage for the straight labyrinth, while it was negligible for the stepped one. Also, they found that for large clearances, the stepped labyrinth behaves with a higher performance than the straight one, which is not the case for small clearances.

Wang et al. [8] tried to find the leakage flow through two labyrinth seals, e.g., interlocking and stepped seals. They used the CFD approach with the k-ε turbulence model and depicted the streamline pattern, velocity vector field and the distribution of the turbulent kinetic energy and static pressure. They found that at the clearance location of the seal, the turbulent kinetic energy reaches its peak value, while in the bulk region of the cavities it decays fast.

In the present work, the main goal is to examine numerically the leakage behavior of the trapezoidal teeth labyrinth seal. Calculations are performed for a sequential increase in a pair of teeth from n = 1 to 6, tip clearances = 0.5 to 9 mm and pressure ratios of PR = 1.5, 2 and 2.5.

Nomenclatures

L	Length
P	Pressure
T	Temperature
u_i	absolute fluid velocity component in direction x_i
G_k	generation of turbulence kinetic energy
Y_M	contribution of the fluctuating dilatation
E	total energy
k	turbulence kinetic energy

Greeks

ρ	Density
$(\tau_{ij})_{eff}$	deviatoric stress tensor
μ	dynamic viscosity
μ_t	turbulent viscosity
μ_{eff}	effective viscosity
ε	turbulence dissipation rate

Subscripts

eff	Effective
t	Turbulent
I	Direction

2.Problem statement

The system of interest is a two-dimensional labyrinth seal with a trapezoidal tooth with height “h” and tip clearance “s” as shown in Fig.1. The geometrical parameters are presented in Table 1. A pair of teeth includes an upward and a downward tooth. Steady compressible gas flow enters the labyrinth and passes through the teeth. The following assumptions are made:

- The flow is 2-D,
- The walls are in no slip condition,
- The k-ε turbulence model is selected.

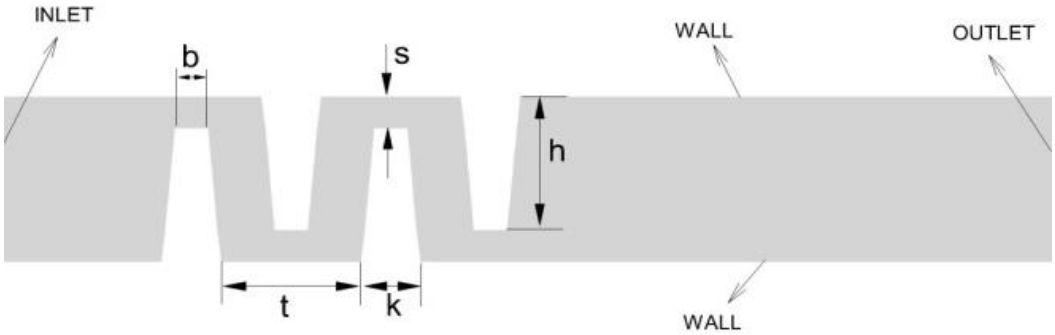

Fig. 1. Schematic diagram of computational set-up

Table 1. The geometrical parameters

Labyrinth Type	n	s (mm)	t (mm)	b (mm)	h (mm)	k (mm)
Trapezoidal	1-6	0.5-9	10.5	2.5	10.5	4.5

3.Governing equations

The flow and heat transfer in the homogeneous flow region inside the trapezoidal labyrinth seal are governed by Navier-Stokes (RANS) and the energy equations, respectively.

$$\frac{\partial}{\partial x_j}(\rho u_j) = 0 \tag{1}$$

$$\frac{\partial}{\partial x_j}(\rho u_i u_j) = -\frac{\partial p}{\partial x_i} + \frac{\partial}{\partial x_j}\left[\mu\left(\frac{\partial u_i}{\partial x_j} + \frac{\partial u_i}{\partial x_i} - 2/3\delta_{ij}\frac{\partial u_l}{\partial x_l}\right) + \frac{\partial}{\partial x_j}(-\rho\overline{u_i}\overline{u_j})\right] \tag{2}$$

$$\frac{\partial}{\partial x_j}\left[u_j(\rho E + p)\right] = \frac{\partial}{\partial x_j}\left[\left(k + \frac{c_p\mu_t}{Pr_t}\right)\frac{\partial T}{\partial x_j} + u_i(\tau_{ij})_{eff}\right] + S_h \tag{3}$$

where,

$$(\tau_{ij})_{eff} = \mu_{eff}\left(\frac{\partial u_j}{\partial x_i} + \frac{\partial u_i}{\partial x_j}\right) - \frac{2}{3}\mu_{eff}\frac{\partial u_l}{\partial x_l}\delta_{ij} \tag{4}$$

$$p = \rho RT \tag{5}$$

The Boussinesq hypothesis [9] is employed to relate the Reynolds stress as:

$$-\rho\overline{u_i}\overline{u_j} = \mu_t\left(\frac{\partial u_j}{\partial x_i} + \frac{\partial u_i}{\partial x_j}\right) - \frac{2}{3}(\rho k + \mu_t\frac{\partial u_l}{\partial x_l})\delta_{ij} \tag{6}$$

The RNG-based k-ε turbulence model is derived from the instantaneous Navier-Stokes equations, using a mathematical technique called the "renormalization group" (RNG) method. A more comprehensive description of the RNG theory and its application to turbulence can be found in [10].

Transport equations for the RNG k-ε Model are:

$$\frac{\partial}{\partial x_j}(\rho k u_j) = \frac{\partial}{\partial x_j}\left(\alpha_k\mu_{eff}\frac{\partial k}{\partial x_j}\right) + G_k + \rho\varepsilon - Y_M \tag{7}$$

$$\frac{\partial}{\partial x_j}(\rho k u_j) = \frac{\partial}{\partial x_j}\left(\alpha_k\mu_{eff}\frac{\partial k}{\partial x_j}\right) + G_k + \rho\varepsilon - Y_M \tag{8}$$

The production of turbulence kinetic energy is defined as:

$$G_k = -\rho\overline{u_i}\overline{u_j}\frac{\partial u_l}{\partial x_l} \tag{9}$$

The dilatation dissipation term,Y_M, is included in the k equation. This term is modeled according to a proposal by Sarkar [11].

$$Y_M = 2\rho\varepsilon M_t M_t = \sqrt{\frac{k}{\gamma RT}} \tag{10}$$

More details about the above-mentioned governing equations are found in Ref. [12, 13].

The pressure ratio "PR" is defined as the inlet total pressure to the exit static pressure. It can be presented as the following equation:

$$PR = \frac{P_{o,in}}{p_{out}} \tag{11}$$

The discharge coefficient, CD, is a description for the seal performance and is formulated as follows:

$$Q_{id} = \sqrt{\frac{2\gamma}{R(\gamma-1)}\left[(\frac{p_{out}}{P_{o,in}})^{\frac{2}{\gamma}} - (\frac{p_{out}}{P_{o,in}})^{\frac{\gamma+1}{\gamma}}\right]} \tag{12}$$

$$\dot{m}_{id} = Q_{id}\frac{A_C P_{o,in}}{\sqrt{P_{o,in}}} \tag{13}$$

$$CD = \frac{\dot{m}}{\dot{m}_{id}} \tag{14}$$

4.Numerical methodology and boundary conditions

The flow governing the equations of (1)-(12) with the pertinent boundary conditions are solved numerically by a Finite-Volume solver. The staggered grid is employed where the velocity components are stored at the cell faces, while the pressure and the temperature are stored at the cell center. Also, the SIMPLE algorithm is utilized for the pressure-velocity de-coupling and iteration [14]. The discretization of the governing equation is accomplished by means of the second-order upwind scheme (SOU). Lower under-relaxation factors ranging from 0.2 to 0.5 had been chosen in order to find a high accuracy in computation. For convergence, the solution is continued until the residuals reach below 10^{-6} for all the equations.

The following boundary conditions are used:

- Inlet flow with specified total pressure and temperature,
- No slip condition at the walls parallel with adiabatic walls,
- Outlet flow with specified static pressure.

5.Grid Independency

Mesh generation for the computation of the fluid flow is a paramount parameter. Therefore, an effort has been made to generate a proper mesh in the mentioned domain. Figure 2 shows the mesh distribution along the computational domain for the case of the two-teeth labyrinth seal. The gird has been stretched with a specific dense grid near the wall and the teeth. To ensure a grid-independent solution, the analysis is performed for various grid sizes and the changes in the discharge coefficient relative to the previous one are presented in Table 2. The grid size with 60000 cells is almost suitable for this computation.

6.Validation

To benchmark the validity of the numerical method, the obtained results of the discharge coefficient with the number of teeth for a straight labyrinth seal are compared with those of Kim and Cha [7] in Fig. 3. The comparison shows a good agreement.

7.Results and discussion

The model is used to demonstrate the flow inside the labyrinth seal with a new geometry of the trapezoidal teeth. The solution is given for the following range of parameters:

- Number of teeth n=1 to 6 with step 1,
- Tip clearance s=0.5 to 9,
- Pressure ratio PR=1.5, 2 and 2.5.

The results of the velocity and total pressure contours, streamline patterns and the variation of the discharge coefficient is obtained.

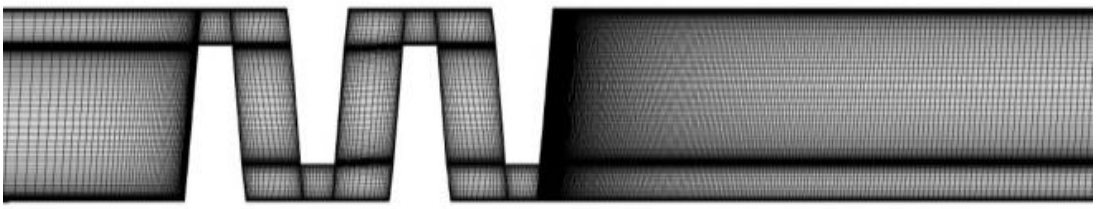

Fig.2. Mesh distribution along the computational domain

Table 2. The effect of grid size on discharge coefficient

No.	Grid size	CD	Changes %
1	5000	0.2516	--
2	10000	0.2458	2.4
3	20000	0.2410	2.0
4	40000	0.2357	1.5
5	60000	0.2350	0.35

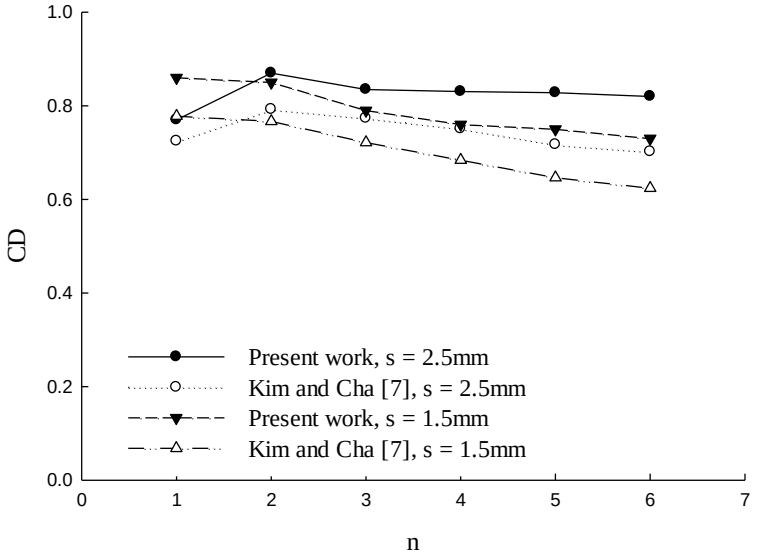

Fig. 3. Comparison of present model results with those of Kim and Cha [7].

The variation of the discharge coefficient (CD) against the number of teeth (n) for various values of the tip clearance (s), shown in Fig. 4, indicates that an increase in n causes a decrease in CD due to a resistance from the added teeth as an obstacle in the flow. As it is seen, the maximum value of CD is at the least s. All the three seals, s=0.5, 1.5 and 2.5, show a decreasing trend in CD when n increases. This is in conformity with the behavior of the other labyrinth types.

To clarify the effect of n on the flow inside the seal, Fig. 5 has been developed for n=2, 4 and 6. The total pressure, x-velocity contours and the streamline pattern has been shown. According to the total pressure contour, its value sharply falls at the first tooth from440000 to 430000 Pa. This is while the losses in the remaining teeth are much lesser.Therefore, the first cavity plays a major role in determining the leakage flow.

In the same results, the increase in n exerts a great influence on the x-velocity distribution throughout the labyrinth. The maximum x-velocity values after the last tooth are around 220, 140 and 120 m/s for the labyrinth seals with n=2, 4 and 6, respectively. In the third part of the Figure, a streamline pattern has

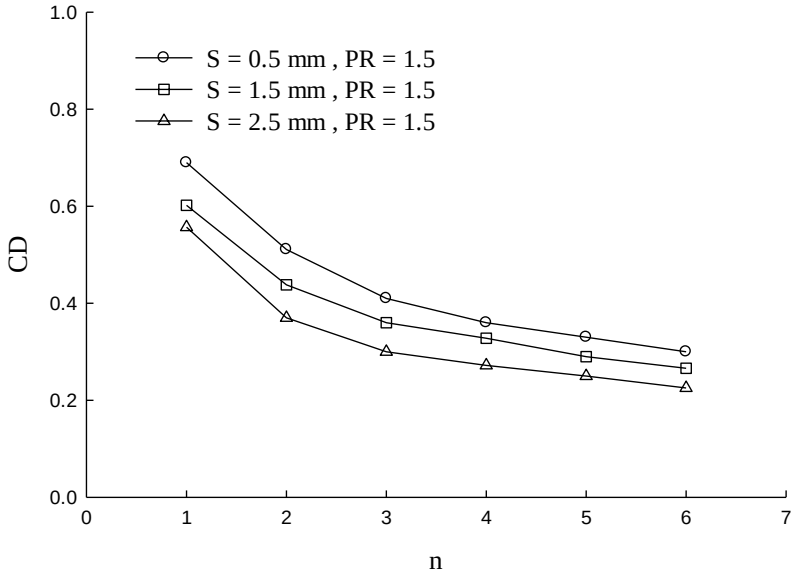

Fig. 4. The variation of CD against number of teeth at fixed PR=1.5

been demonstrated in order to show the flow vertical motion through the trapezoidal tooth inside the seals. It is obviously observed that there are some vortices on the teeth left wall. But there is a non-negligible point that the created vortices are larger than the vortices in the labyrinth with normal teeth (straight) presented in Ref [7]. So, these vortices have a significant effect on the discharge coefficient. One of the important parameters that influences the discharge coefficient is the tip clearance. The variation of CD against s is given in Fig. 6. It is observed that an increase in s from 0.5 mm to around 7.5 mm leads to a decrease in the leakage, but a reverse behavior for an increase beyond 7.5 mm. To explain this dual behavior with the increasing s, in particular the abrupt change of CD around s=7.5 mm, the contours of total pressure, x-velocity component and the streamline pattern are shown in Fig. 7 for various values of clearance sizes s=1.5, 2.5 and 4.5 mm. At a given point, the total pressure increases with an increase in s for all the seals and also the maximum x-velocity for s=4.5 mm is more than the others. In the streamline pattern, by increasing the s, the created vortices get stronger around the tooth and act as a resistance to the flow and result in a decrease in the leakage flow. This phenomenon is obviously seen in Fig. 7 (c). For the value of s is larger than 7.5 mm, the vortices tend to be smaller and hence, the clearance behavior changes.

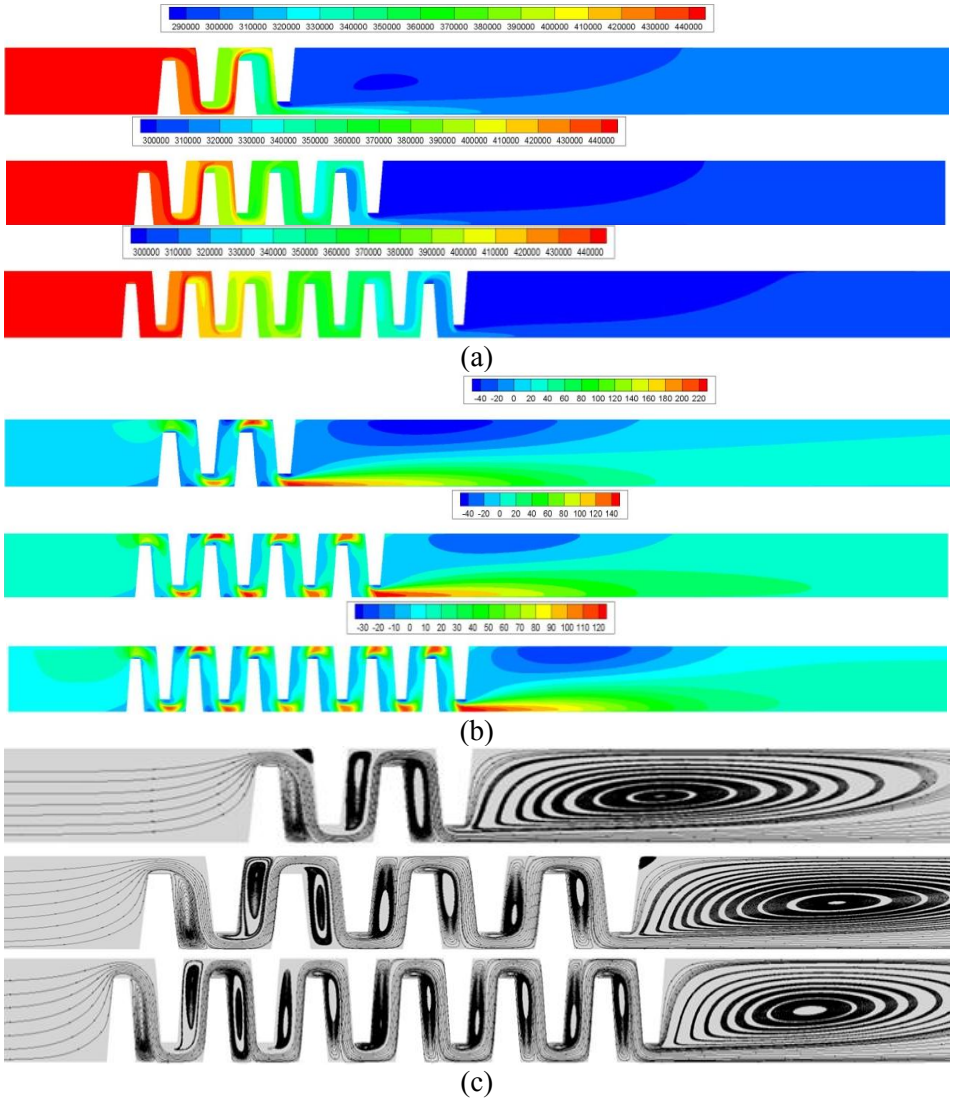

Fig.5. Contours of a) total pressure, b) x-velocity component, and c) streamline pattern for trapezoidal labyrinth seal with n=2, 4 and 6 at fixed PR=1.5

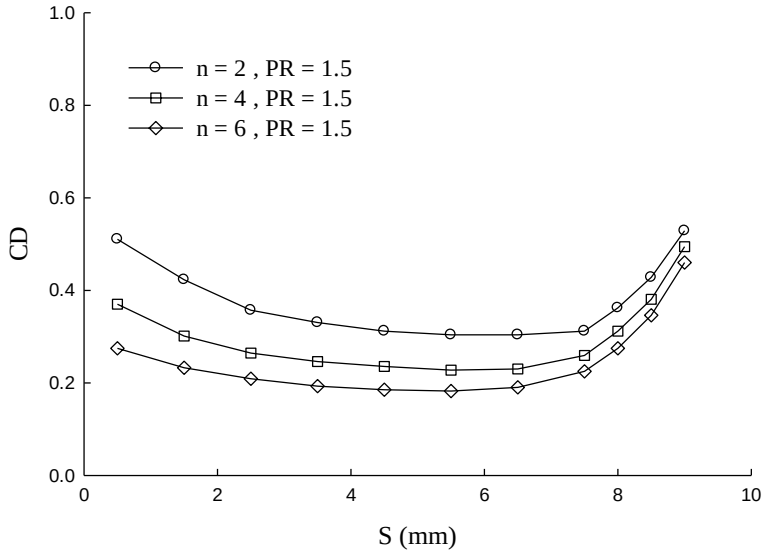

Fig. 6. Effect of s on Cd for different n at fixed PR= 1.5

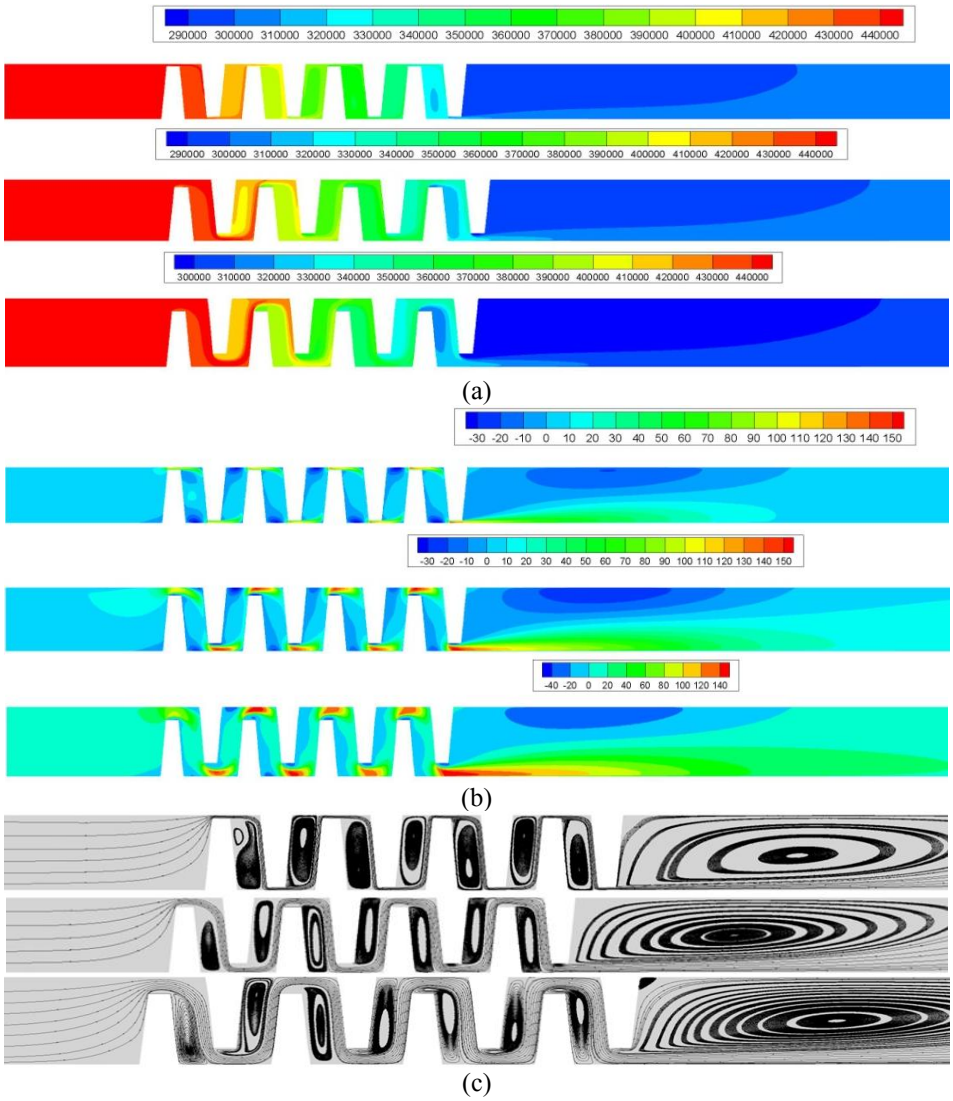

Fig. 7. Contours of a) total pressure, b) x-velocity component, and
c) streamline pattern for trapezoidal labyrinth seals with s=0.5, 1.5 and 2.5 mm at fixed PR=1.5 and n=4

Pressure ratio is an appropriate mean for controlling the leakage flow inside the labyrinth seal. Increase in PR causes an increase in CD. This fact has been established clearly in Fig. 8 as a variation of CD against n for different PR values. These results are in conformity with the results of Refs [7, 8].

8.Conclusion

The present work is an attempt to investigate the effect of the geometrical parameters on the leakage flow through the trapezoidal labyrinth seal, including the number of teeth, n, pressure ratio, PR and the tip clearance, s. A Finite-Volume solver is used to simulate the leakage flow inside the labyrinth seal.
The obtained results can be summarized as follows:

- As expected, an increase in the number of teeth causes a decrease in the discharge coefficient due to the applied larger resistance to the flow. The maximum fall in CD occurs around n=2 as the highest reduction in the total pressure occurs just after the first tooth.
- The tip clearance is a small gap for passing the fluid. Hence, an increase in s causes a decrease in CD. This is in contrast with the behavior of the straight labyrinth, but is in conformity with the step labyrinth. For s=0.5 to 7.5 mm, an increase in S causes a decrease in CD due to the fact that the created vortices around the teeth get bigger, so these vortices ricochet off the tooth and act as a resistance to the flow and result in a decrease in the leakage flow.
- For s> 7.5 mm, an increase in s causes a positive effect on CD.
- The pressure ratio has a positive effect on CD, an increase in the results of which leads to an increase in the leakage flow, as expected.

References

[1] Chupp R. E., Hendricks R. C., Lattime S. B., Steinetz B. M., Sealing in Turbomachinery, Journal of Propulsion and Power (2006) 22(2): 313-349.
[2] Stoff H., Incompressible Flow in a Labyrinth Seal, The Journal of Fluid Mechanics (1980)100: 817-829.
[3] Rhoded L., Demko J. A., Morrison G. L., On the Prediction of Incompressible Flow in Labyrinth Seals. ASEM Journal of Fluids Engineering (1984)108(1):19-25.
[4] Malvano R., Vatta F., Vigliani A., Rotordynamic Coefficients for Labyrinth Gas Seal, Single Control Volume Model. Meccanica (2001) 36(66): 731-744.
[5] Rhode D. L., Johnson J. W., D. H. Broussard, Flow Visualization and Leakage Measurements of Stepped Labyrinth Seals, Part1 – Annular Groove,

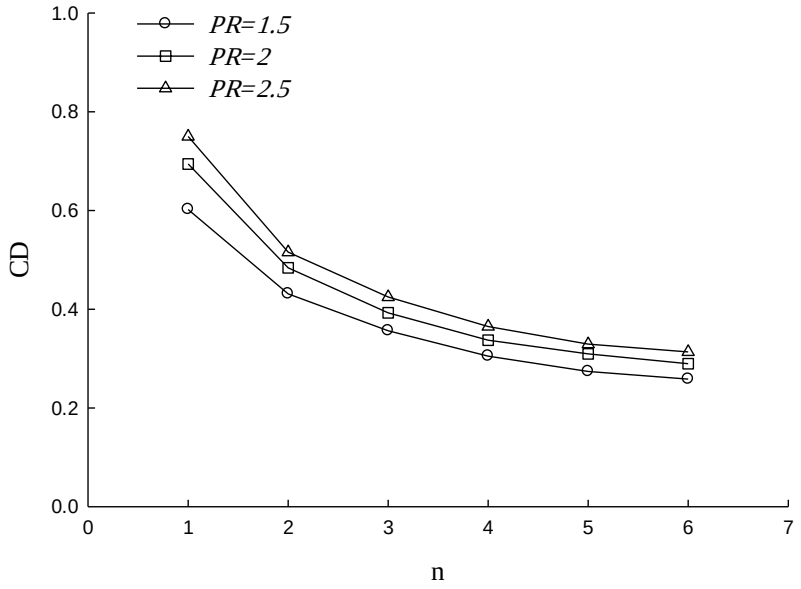

Fig. 8. Variations of Cd against n for different PR and s=2.5mm

ASME Journal of Turbomachinery (1997)119(4): 839-843.

[6] Vakili A. D., Meganathan A. J., Michaud M., Radhakrishnan S., An Experimental and Numerical Study of Labyrinth Seal Flow, ASME Paper Gas Turbine 2005-68224 (2005).

[7] Kim T. S., Cha K. S., Comparative Analysis of the Influence of Labyrinth Seal Configuration on Leakage Behavior, Journal of Mechanical Science and Technology (2009) 23: 2830-2838.

[8] Wang W., Liu Y., Jiang P., Chen H., Numerical Analysis of Leakage Flow Through Two Labyrinth Seals, Journal of Hydrodynamics (2007)19(1):107-112.

[9] Hinze J. O., Turbulence, McGraw-Hill Publishing Company, New York (1975).

[10] Choudhury D., Introduction to the Renormalization Group Method and Turbulence Modeling, Fluent Incorporated Technical Memorandum, TM-107 (1993).

[11] Sarkar S., Balakrishnan L., Application of a Reynolds-Stress Turbulence Model to the Compressible Shear Layer, ICASE Report 90-18, NASA CR 182002 (1990).

[12] FLUENT 6.3 User's Guide, Fluent Incorporated (2006).

[13] Bovand M., Valipour M. S., Eiamsa-ard S., Tamayol A., Numerical Analysis for Curved Vortex Tube Optimization, International Communications in Heat and Mass Transfer (2013) 50:98-107.

[14] Patankar S.V., Numerical Heat Transfer and Fluid Flow, Hemisphere, New York (1980).